Physica Scripta

PAPER

Study of ferromagnetism and thermoelectric behaviour of thiospinels $MgFe_2(S/Se)_4$ for spintronics and energy harvesting

Syed Awais Rouf[1], **Nasreen Akhtar**[2], **Nessrin A Kattan**[3], **Jameelah Alzahrani**[4,5], **Q Mahmood**[4,5], **Samah Al-Qaisi**[6], **Manal Morsi**[7,8], **Hind Albalawi**[9], **Sarah Alharthi**[10], **Mohammed A Amin**[10] and **H H Somaily**[11,12]

[1] Department of Physics, Division of Science and Technology, University of Education, Lahore, Pakistan
[2] Department of Physics, Chenab College Jhang, Jhang, Pakistan
[3] Department of Physics, College of Science, Taibah University, Medina, Saudi Arabia
[4] Basic and Applied Scientific Research Center, Imam Abdulrahman Bin Faisal University, P O Box 1982, 31441 Dammam Saudi Arabia
[5] Department of Physics, College of Science, Imam Abdulrahman Bin Faisal University, P O Box 1982, 31441, City Dammam, Saudi Arabia
[6] Palestinian Ministry of Education and Higher Education, Nablus, Palestine
[7] Department of Physics, College of Arts and Science, Wadi Addawasir, Prince Sattam bin Abdulaziz University, Saudi Arabia
[8] Department of Physics, Girl College for Art, Science, and Education, Ain-Shams University, Cairo, Egypt
[9] Department of Physics, College of Sciences, Princess Nourah bint Abdulrahman University (PNU), P O Box 84428, Riyadh, 11671, Saudi Arabia
[10] Department of Chemistry, College of Science, Taif University, P O Box 11099, Taif 21944, Saudi Arabia
[11] Research Center for Advanced Materials Science (RCAMS), King Khalid University, Abha 61413, P O Box 9004, Saudi Arabia
[12] Department of Physics, Faculty of Science, King Khalid University, P O Box 9004, Abha, Saudi Arabia

E-mail: syedawais.rouf@ue.edu.pk

RECEIVED
31 March 2022

REVISED
13 September 2022

ACCEPTED FOR PUBLICATION
30 September 2022

PUBLISHED
13 October 2022

Keywords: spinels, ferromagnetism, thermoelectric, behaviour, thiospinels, $MgFe_2(S/Se)_4$

Abstract

Magnesium-based spinel chalcogenides are remarkable materials for spintronic and energy harvesting applications. Therefore, the electronic, ferromagnetism, and thermoelectric characteristics of $MgFe_2(S/Se)_4$ spinels are addressed comprehensively by modified Becke Johnson potential (TB-mBJ). The stability of cubic phase has been illustrated by formation energy and energy released during optimization. The Curie temperature and spin polarization have been calculated by Heisenberg model and density of states at Fermi level. Ferromagnetism has been studied by exchange energies, double exchange mechanism, exchange constants, and hybridization process. The reduction of magnetic moment of Fe and its shifting on nonmagnetic (Mg, S/Se) sites shows the ferromagnetism is due to the exchange of electrons spin rather than the clustering effect of internal magnetic of Fe atoms in the structure. Moreover, thermoelectric analysis of studied spinels has been illustrated by electrical and thermal conductivities, Seebeck coefficient (S), and power factor.

1. Introduction

Chalcogenide spinels, having large colossal magnetoresistance (CMR), giant magnetoresistance, and magnetoelectric effect are the leading parameters for spintronics. The ferromagnetic semiconductor materials contain semiconducting nature in one spin channel and insulating nature in another spin channel with complete spin polarization (SP). The SP is essential for reducing heat problems of ICs and other electronic devices. Therefore, the materials having a significant magnetic moment, phase transition temperature, and spin polarization are considered important to boost the spintronic technology like magnetic random access memories (MRAM), magnetic switches, spin valves, magnetic sensors, and magnetic recorders [1–3].

In last few decades, various materials like dilute magnetic semiconductors, Heusler alloys, transition metal oxides, Perovskites, double perovskites, and spinel's have been elaborated vastly for spintronic applications [4–10]. For ferromagnetic semiconductors of type AB_2X_4 with high Curie temperature has been remained the primary consideration of researchers [11]. The geometrical distortion of these materials creates magnetic frustration, which can be overcome by the exchange mechanism [12–14]. The combination of magnetic and

semiconductor nature of these spinels is the main subject of research because of their technological spintronic applications. Furthermore, the existence of colossal magnetoresistance in these ferromagnetic spinels boosted their demand for spin based technology [15].

The magnesium chalcogenides $MgCr_2(S/Se)_4$ exhibit ferromagnetic nature with a substantial negative magnetoresistive effect which is close to their Curie temperature [16]. The transition temperature of $CdCr_2S_4$ and $CdCr_2Se_4$ were recorded as 84.5 K and 129.5 K, respectively [17]. Wustrow *et al* [18] had also been studied another Mg-based thiospinel, $MgCr_2S_4$, to tackle the high voltage Cr3þ/Cr4þ couple. The high voltage coupling effect and divalent Mg ion had reduced the value of diffusion barrier and asserted to soft anionic lattice system [19]. Nazar *et al* [20] described the interpolation mechanism of Mg ion with Ti-based thiospinels at different temperatures and found fruitful results for electrochemical recycling. The Colossal Magnetoresistance in ferro-spinels introduces a fascinating platform for researchers to explore the ferromagnetism [21, 22]. Therefore, the $MgCr_2S_4$ and $MgMn_2S_4$ are outstanding ferromagnets because of complete spin polarization and large magnetic moments of Mn and Cr [23, 24]. Furthermore, Mehmood *et al* described the magnetic and thermoelectric characteristics of $MgPr_2(S/Se)_2$ for spintronics by DFT based analysis [25].

The literature on spinel's $MgFe_2(S/Se)_4$ about HM ferromagnetism and thermoelectric properties is limited. Therefore, in the present article, we have comprehensively addressed the electronic structure, spin polarization, Curie temperature, HM ferromagnetism, and thermoelectric characteristics of Mg-based thiospinels $MgFe_2(S/Se)_4$. The main findings are ferromagnetism due to exchange mechanism and complete spin polarization without clustering of Fe. The BoltzTrap code probes the thermoelectric properties because thermal conductivity and temperature significantly influence the spin polarization that reduces the device's life. Therefore, thermoelectric influence on spin polarization is elaborated comprehensively.

1.1. Method of calculations

The full potential-linearized augmented plane wave (FP-LAPW) method have been applied to elaborate the electronic behavior and ferromagnetism in $MgFe_2S_4$ and $MgFe_2Se_4$ using Wien2k software [26]. The GGA approximation and TB-mBJ exchange potential have been used to explore ferromagnetic properties. Because the TB-mBJ potential calculates the accurate electronic band gap [27]. Generally, the spherical harmonics inside muffin-tin spheres and plane waves in interstitial regions have been used for analysis. For energy convergence, the value of $R_{MT} \times K_{max} = 8$ and $G_{max} = 24\ Ry^{-1}$ are used. Energy convergence criteria are set up to 0.00001 Ry to obtain the best convergence. The k-mesh of $12 \times 12 \times 12$ has been incorporated for both band structures and the density of states. Finally, the BoltzTraP code is employed to evaluate the thermoelectric properties [28].

2. Results and discussion

2.1. Structural properties

The cubic crystal structures of the studied spinels, $MgFe_2(S/Se)_4$ with space group 227_$Fd\bar{3}m$ has been shown in figure 1. The cubic unit cell of the spinel structures contains 56 atoms in which 32 atoms of S/Se formed FCC lattice, which occupies the tetrahedrons and octahedrons of Mg and Fe atoms. Each corner of tetrahedrons shared (1/8) to 8 atoms of Mg and 16 atoms of Fe shared to octahedrons (1/2). The atomic coordinates Mg (1/8, 1/8, 1/8), Fe (1/2, 1/2, 1/2), and S/Se (1/4, 1/4, 1/4) are used according to the mentioned space group. To relax the cubic structures, the strain present among atom inside the structures has been reduced to 0.0001 GPa. After relaxing the structures, the energies in ferromagnetic (FM), anti-ferromagnetic (AFM), and paramagnetic (PM) states are noted to confirm the most favorable and stable state. The energy versus volume graphs in AFM, FM, and PM states are presented in figures 2(a), (b). The lowest ground state energy in the FM state confirms the stability of $MgFe_2X_4$ (X = S, Se). The bulk modulus and lattice parameters of $MgFe_2X_4$ (X = S, Se) compounds have been computed by the fitting equation of state [29] to total energy versus volume data. The calculated values for structural properties have been given in table 1. The low Curie temperature (T_c), increase in lattice parameters from 10.28 to 10.79 is due to an increase anionic radii from 1.700 Å and 1.840 Å for S and Se, respectively. In contrary to this decrease in covalent character between cations and anions can be attributed to larger atomic radius and smaller electronegativity of selenium (Se).

Furthermore, the decrease in hardness from $MgFe_2S_4$ to $MgFe_2Se_4$ is due to increase of bulk modulus. It is reported that the $MgFe_2S_4$ [30] and $MgFe_2Se_4$ [31, 32] are more stable than other possible magnesium-based chalcogenides. To support the above statement the formation energy has been calculated by the relation

$$\Delta H_f = E_{Total}(Mg_lFe_m(S/Se)_n) - lE_{Mg} - mE_{Fe} - nE_{S/Se} \quad (1)$$

Where $E_{Total}(Mg_lFe_mS/Se_n)$ is the total energy, (E_{Mg}, E_{Fe} and $E_{S/Se}$) are the energies of (Mg, Fe, and S/Se) atoms. The calculated values of ΔH_f are reported in table 1, whose negative sign ensure the thermodynamic

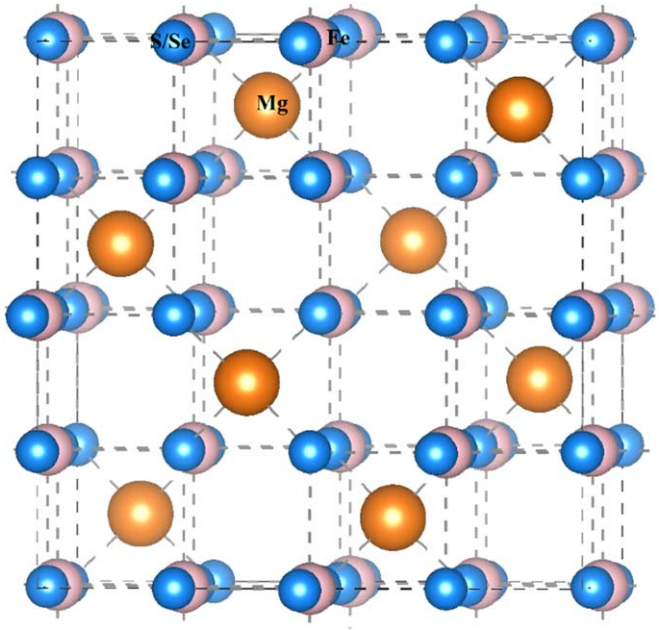

Figure 1. Crystal structure of $MgFe_2(S/Se)_4$, [Fe: pink color, Mg: yellow color, S/Se: blue color].

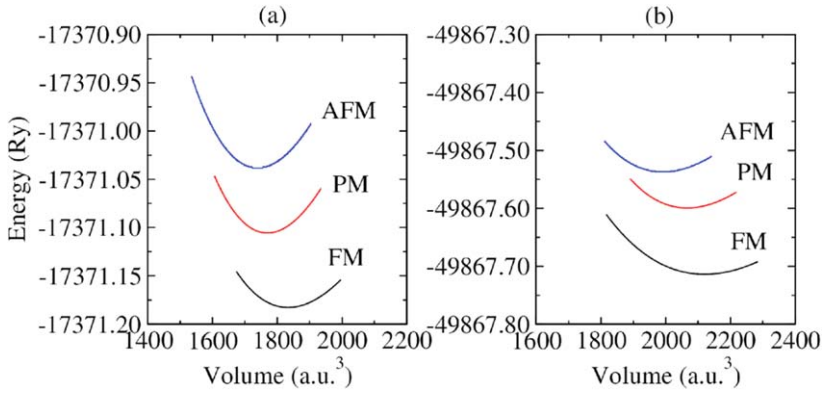

Figure 2. Energy (Ry) versus Volume (a. u.) plots of (a) $MgFe_2S_4$ and (b) $MgFe_2Se_4$ in PM, FM, and AFM states.

Table 1. The computed ground state parameters, Curie temperature, and spin polarizations.

Parameters	$MgFe_2S_4$	$MgFe_2Se_4$
Lattice constant a (Å)	10.28	10.79
Bulk modulus B (GPa)	67.46	56.18
Curie temperature T_c (K)	331	302
Formation energy ΔH_f (eV)	−2.30	−2.15
Up spin density N (↑)E_F	0.00	0.00
Down spin density N (↓)E_F	0.10	0.10
Spin polarization SP	1.00	1.00

stability in FM states [33]. Moreover, the Curie temperature has been found by Classical Heisenberg model analysis through the relation $Tc = \Delta E/3K_B$, where K_B is constant, and ΔE is the energy difference of AFM and FM states [34]. The computed Tc in table 1 ensures the room temperature ferromagnetism which is mandatory for advanced spintronic technology. Furthermore, for the studied magnetic system, the spin-polarized density of states is computed by relation

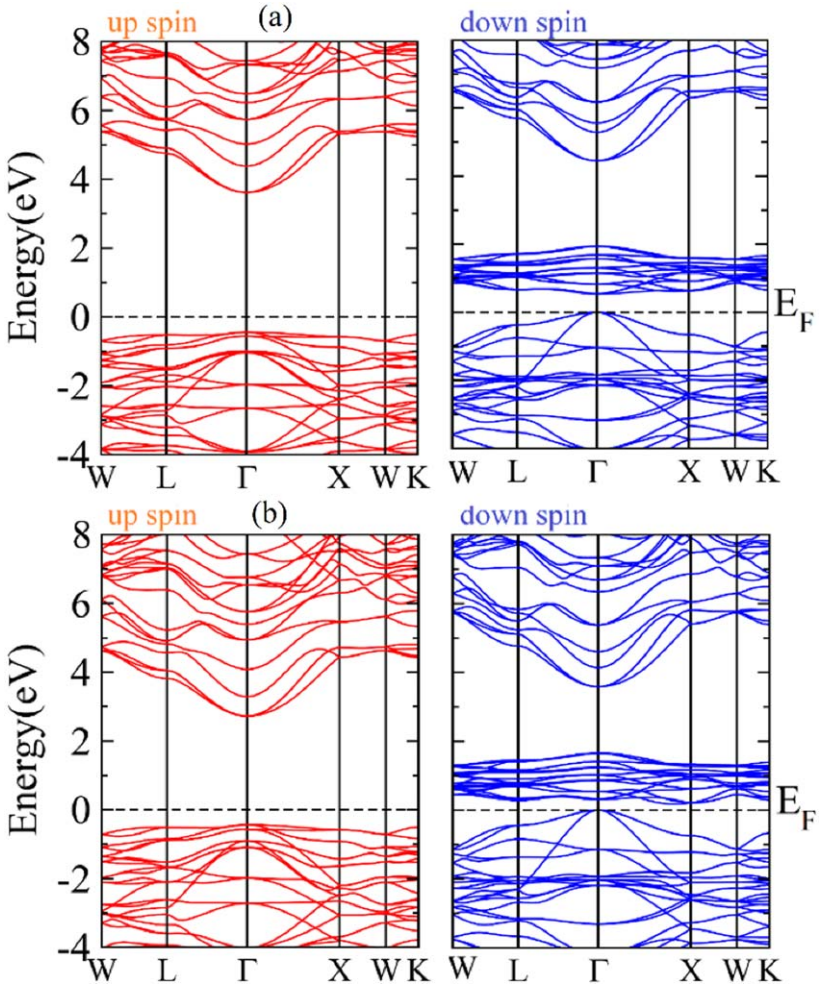

Figure 3. Band structure of (a) $MgFe_2S_4$ and (b) $MgFe_2Se_4$.

$$SP = \frac{N(\uparrow)E_F - N(\downarrow)E_F}{N(\uparrow)E_F + N(\downarrow)E_F} \times 100\% \quad (2)$$

Where the density of states ($N(\uparrow)$, $N(\downarrow)$) are computed at the Fermi level for both spinel channels (↑ & ↓). The calculated SP density ensures the 100% spin polarization at E_F, which is the important factor of studied spinels for spintronics [35].

2.2. Electronic properties

For the study of electronic properties, discussion about the band gap and density of states is a matter of keen interest. The Mg-based spinels show an interesting electronic property to elucidate ferromagnetism. The evaluation of correct band gap is essential because it helps to explore physical properties accurately. For this purpose, TB-mBJ potential has been used to predict correct band gap of studied materials [36]. The calculated BS with the help of this technique are represented in figures 3(a), (b). A Fermi level (zero energy level) is represented with horizontal dotted lines between the conduction and valence band. The valence band maxima and conduction band minima meet at Γ point in both spin channels. Hence, it is justified that both the spinels, $MgFe_2X_4$ (X = S, Se), exhibit direct band gaps. The BS shows the up-spin channel is insulating and down spin channel is semiconducting.

For spin up channel, the states are near the E_F in valence band maxima and away in conduction band minima for $MgFe_2X_4$ (X = S, Se). In spin down channel, the valence states are present at E_F, and conduction states are near E_F, which form the narrow band gap as shown in figures 3(a), (b). Hence, change in anion can affect the BS of the studied compound, revealing its potential applications and importance [37]. The movement of E_F discriminates the up spin as insulating and down spin as a semiconductor, leading to the combined effect as ferromagnetic semiconductors.

Furthermore, for the detailed discussion of DOS, the density of states is elaborated in figures 4(a), (b). The TDOS exhibits a ferromagnetic nature similar as BS. In usual trends of ferromagnetic semiconductors, spin up

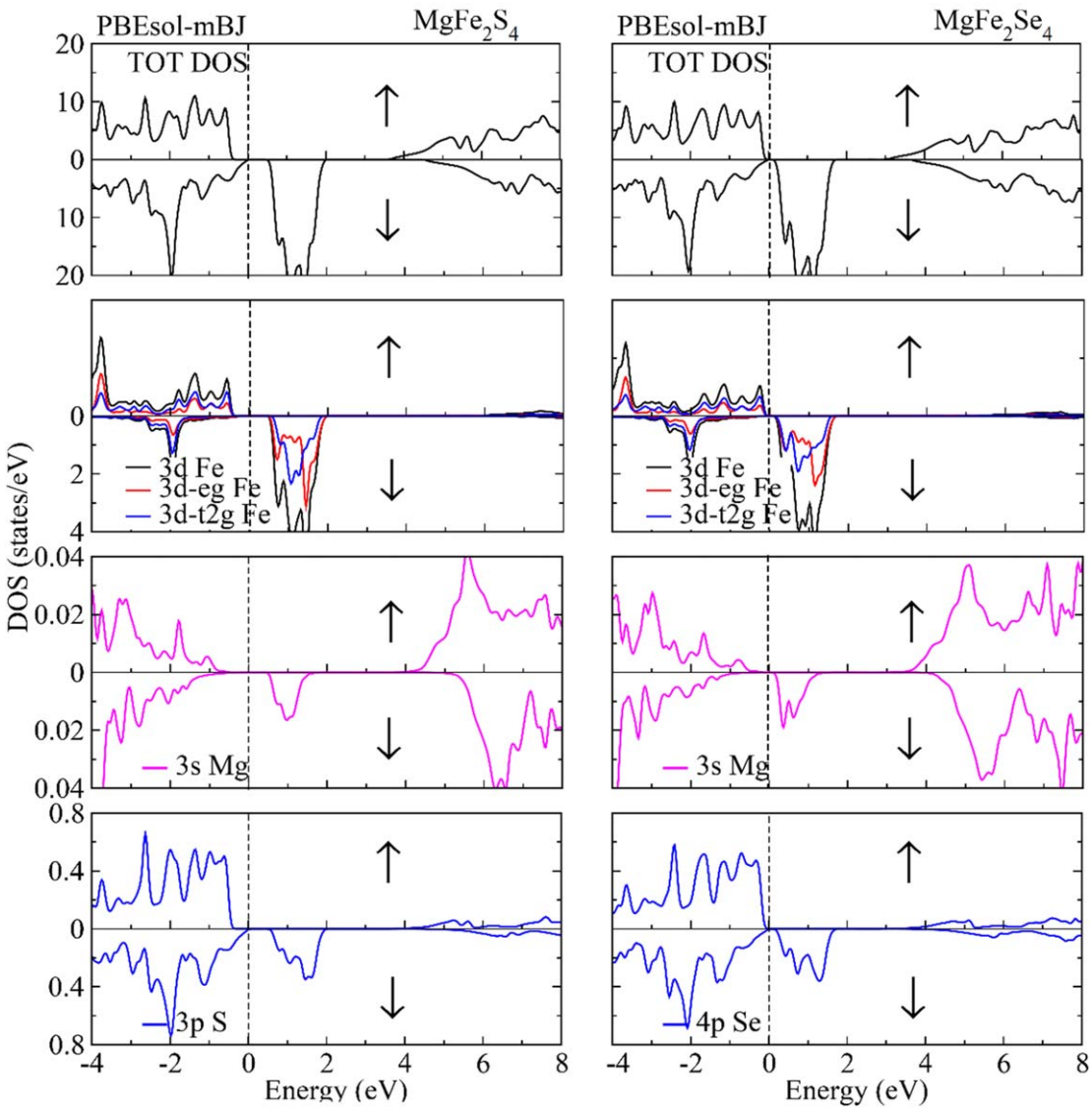

Figure 4. The density of states of $MgFe_2S_4$ and $MgFe_2Se_4$.

behaves as a semiconductor and spin down as an insulator because of the exchange mechanism. Here, in the present case, the spin-up and spin-down states are reverted due to the quantum confinement effect in which wave functions of electrons are bound in the quantum well [38]. A strong hybridization exists between Fe-3d and S/Se-p states, which manipulate ferromagnetic interaction [39]. In lower energy region, −4 eV to −1 eV, 3d-$e_{.g.}$ states are highly contributed to spin up channel as compared to spin down channel. In upper energy region, the 3d-$e_{.g.}$ states are highly contributed to hybridization for $MgFe_2S_4$, but their contribution reduces as anion changes from S to Se. If we discuss the 3d-t_{2g} states, their contribution is almost identical for both anions, as discussed in the upper energy region 0.3 eV–1.7 eV (see figure 4). The crystal field splits Fe-3d states into 3d-$e_{.g.}$ and 3d-t_{2g} states. The 3d-$e_{.g.}$ states are doubly degenerate and 3d-t_{2g} states are triply degenerate. The 3d-$e_{.g.}$ states move to higher energy, and 3d-t_{2g} states move to lower energy levels. Therefore, the energy difference 3d-t_{2g}-3d-$e_{.g.}$ is measured as crystal field energy $\Delta_{CF,}$ which tries to frustrate ferromagnetism.

The direct exchange energy $\Delta(d)$ is measured by the energy difference of 3d states of Fe in spin up and spin down states by the relation $\Delta(d) = \Delta(d^{\downarrow}) - \Delta(d^{\uparrow})$. The computed values of $\Delta(d)$ are presented in table 2. By making a comparison between $\Delta(d)$ and Δ_{CF}, it is observed that $\Delta(d)$ has more values than $\Delta_{CF,}$ which is evident that ferromagnetism is due to the exchange of electrons [40]. Another factor is that the indirect exchange energy comes from the exchange of electrons of p states of anions (S/Se) and 3d states of cations (Fe). The computed values from DOS are presented in table 2. Its values are noted from the position of p-states of S/Se in down spin channel. The $\Delta(pd)$ increases as the anion changes from S to Se which make the studied spinel's excellent for spintronic applications. The lowering of energy of the system by exchange mechanism and negative $\Delta(pd)$ are exactly according to the exchange mechanism and Zener's model, which illustrate ferromagnetism

Table 2. Computed exchange energies, exchange constants, and magnetic parameters.

Parameters	$MgFe_2S_4$	$MgFe_2Se_4$
crystal field energy Δ_{CF}	0.40	0.50
direct exchange energy $\Delta(d)$	1.72	1.02
indirect exchange energy $\Delta(pd)$	−0.58	−0.22
exchange constant (sd) $N_o\alpha$	0.855	0.703
exchange constant(pd) $N_o\beta$	−0.027	−0.037
Total MM (μ_B)	4.000	4.000
Int MM(μ_B)	1.388	1.696
Mg MM(μ_B)	0.022	0.023
Fe MM(μ_B)	3.941	3.863
X (X = S, Se) (μ_B)	0.350	0.351

due to transition metals [41–43]. The studied thiospinels $MgFe_2(S/Se)_4$ are also the ideal candidates band gap engineering.

2.3. Magnetic properties

To understand the magnetic properties the magnetic moments of studied spinel's are taken in Bohr magneton (μ_B) as presented in table 2. According to Hund's rule and Pauli exclusion principle, the magnetic moment (MM) is calculated from the software. The MM for spinels, individual elements (Mg, Fe, S/Se), and interstitial sites are represented in table 2. The electronic configuration of Fe-3d show 4 partially filled states, therefore, its total MM should be 4 μ_B as described Pauli exclusion principle [44]. The reduction in MM and its growth on interstitial and nonmagnetic sites illustrate the exchange of electrons has been taken place. In the case of $MgFe_2S_4$, MM is reduced from 4 μ_B to 1.33 μ_B, and for $MgFe_2Se_4$ is reduced from 4 μ_B to 1.69 μ_B due to p-d hybridization among p-states of S/Se and Fe-3d states (see table 2). This hybridization causes VB and CB edge splitting which introduce exchange splitting constants like $N_0\alpha$ and $N_0\beta$ [45]. In these exchange constants, $N_0\alpha$ is positive while $N_0\beta$ is negative, which shows the antiparallel alignment of s-d coupling at VB, p-d coupling at CB. Therefore, the exchange constants are calculated by using $N_0\alpha = \Delta E_c/x\langle S\rangle$ and $N_0\beta = \Delta E_v/x\langle S\rangle$, where ΔE_v and ΔE_c are the difference in energies at valence band edges and conduction band edges for both spins. The $\langle S\rangle$ is the average MM of Fe, and x is the concentration of Fe. The negative values of $N_0\beta$ show that the exchange of electrons lowers the energy of studied system to stabilize ferromagnetism when E_F operates through the energy gap region [46, 47].

2.4. Thermoelectric properties

The thermoelectric characteristics of the studied spinels reveal their importance utilization in thermoelectric applications. The thermoelectric parameters of $MgFe_2S_4$ and $MgFe_2Se_4$ are computed using BoltzTraP code and deliberated in figures 5(a)–(d). The electrical conductivity (σ), thermal conductivity (κ), and Seebeck coefficients (S) values are calculated by combining their values for both spin up and spin down channels using following equation

$$\sigma = \frac{\sigma(\uparrow) + \sigma(\downarrow)}{2} \tag{3}$$

$$k = \frac{k(\uparrow) + k(\downarrow)}{2} \tag{4}$$

$$S = \frac{\sigma(\uparrow)S(\uparrow) + \sigma(\downarrow)S(\downarrow)}{\sigma(\uparrow) + \sigma(\downarrow)} \tag{5}$$

The σ shows the motion of free charge carriers, and its value increases by increasing temperature because temperature increase the energy of the free carriers. The increase in σ is minor up to 350 K and then after increases faster at faster rate up to 800 K as illustrated in figure 5(a). The observed σ at 800 K, for $MgFe_2S_4$ is 2×10^4 $(1/\Omega m.s)$, and for $MgFe_2Se_4$ is 2.5×10^4 $(1/\Omega m.s)$. Here, only electronic thermal conductivity (κ_e) has been calculated (figure 5(b)) because the classical theory based BoltzTraP code has limitations. However, total thermal conductivity has two parts, i.e., the electronic (κ_e) and phonon (κ_p) parts. A potential thermoelectric material contained ultralow κ_p [48, 49]. The κ_e rises gradually with the rise in temperature similarly as electrical conductivity but its values extremely low as compared to σ [50]. The comparative analysis of σ and κ ensures that σ is 10^4 times larger than κ_e. Therefore, the studied materials are suitable for energy harvesting and spintronic application.

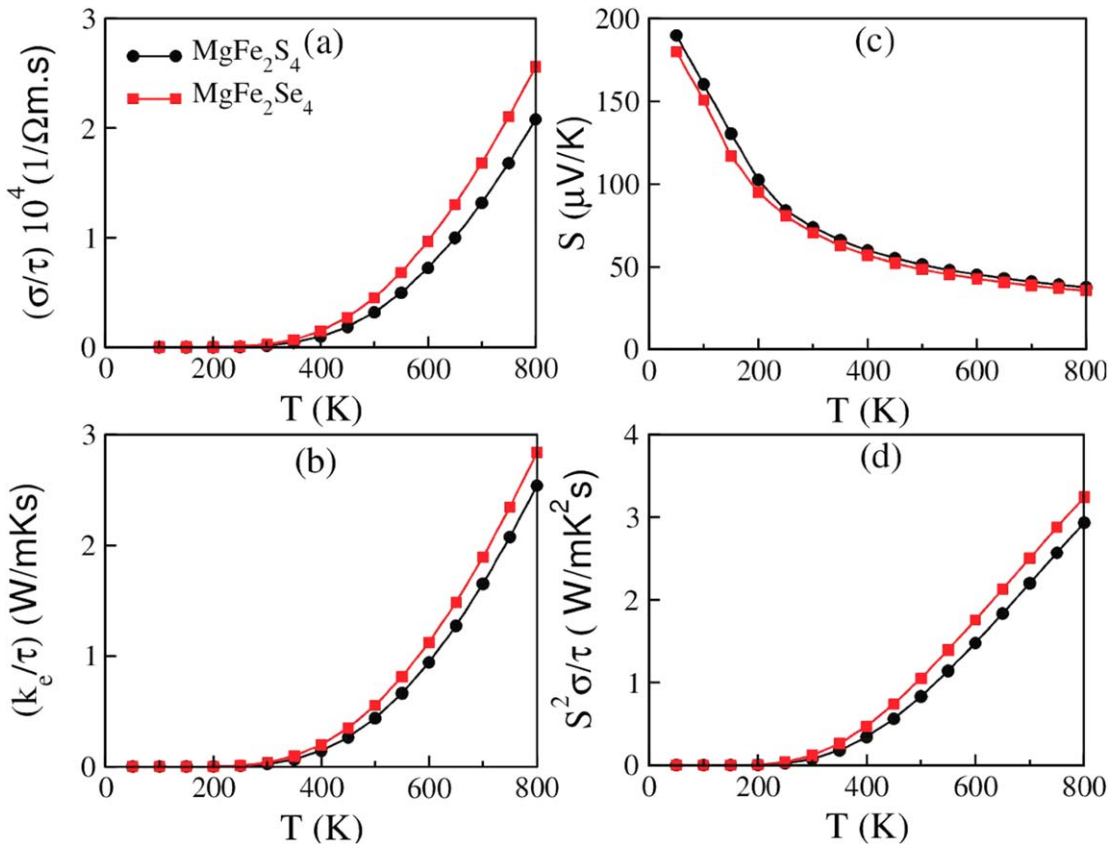

Figure 5. Calculated (a) electrical conductivity, (b) thermal conductivity, (c) Seebeck coefficient (S), and (d) power factor of $MgFe_2(S/Se)_4$ spinels.

The S illustrate about the change in potential due to temperature changes when two dissimilar metals are in contact. At 50 K, S is significant for both $MgFe_2S_4$ and $MgFe_2Se_4$, which rapidly decreases up to 250 K, and after this decrease in S becomes slow up to 800 K. The positive values of S show the studied spinels are semiconductors. The thermoelectric strength of studied spinels is calculated from power factor as presented in figure 5(d). The PF does not include the contribution of thermal conductivity. Its values increase parabolically up to 800 K. The comparative analysis shows $MgFe_2Se_4$ has a more PF than $MgFe_2S_4$ at 800 K. The thermal properties can be improved further by applying external pressure, which directly influences band gap and hence the thermal transports [51, 52].

3. Conclusion

This research work illustrates the detailed study of electronic, magnetic, and thermoelectric properties of $MgFe_2S_4$ and $MgFe_2Se_4$ to explore them for spintronic and energy devices. The lowest energy of FM states as compared to AFM and PM states shows the FM states are more stable. The thermodynamic stability of FM states has been ensured by negative formation energy. The analysis of hybridization and exchange energies from BS and DOS ensure the ferromagnetic semiconducting nature of studied materials. The computed direct exchange energy is more than crystal field energy, which confirms the ferromagnetism is due to electrons spin. Furthermore, the negative Δ(pd) and $N_0\beta$ lower the energy of studied system in FM states because of strong interaction of *p-d* electrons. Furthermore, the large electrical conductivity and ultralow thermal conductivity increases the power factor which make them suitable for thermoelectric applications.

Acknowledgments

The authors would like to thank Taif University Researchers Supporting Project number (TURSP-2020/200), Taif University, Taif, Saudi Arabia for supporting this project. The authors extend their sincere appreciation to the Researchers Supported by the Princess Nourah bint Abdulrahman University Researchers Supporting Project number (PNURSP2022R29), Princess Nourah bint Abdulrahman University, Riyadh, Saudi Arabia. The

authors also extend their appreciation to the Deanship of Scientific Research at King Khalid University for the financial support through the research groups program under grant number (R. G. P. 2/6/43).

Data availability statement

All data that support the findings of this study are included within the article (and any supplementary files).

ORCID iDs

Syed Awais Rouf https://orcid.org/0000-0002-8508-2572
Q Mahmood https://orcid.org/0000-0001-7449-5876
Mohammed A Amin https://orcid.org/0000-0001-5091-0641

References

[1] Hemberger J, Lunkenheimer P, Fichtl R, Nidda H A K, Tsurkan V and Loidl A 2005 *Nature* **434** 364
[2] Ohgushi K, Ogasawara T, Okimoto Y, Miyasaka S and Tokura Y 2005 *Phys. Rev.* B **72** 155114
[3] Assa Aravindh S D, Schwingenschloegl U and Roqan I S 2015 *J. Chem. Phys.* **143** 224703
[4] Roqan I S, Venkatesh S, Zhang Z, Hussain S, Bantounas I and Franklin J B 2015 *J. Appl. Phys.* **117** 073904
[5] Pandey S K 2011 *Phys. Rev.* B **84** 094407
[6] Mounkachi O, Benyoussef A, El Kenz A, Saidib E H and Hlil E K 2009 *Physica* A **388** 3433–41
[7] Goumrhar F, Bahmad L, Mounkachi O and Benyoussef A 2017 *J. Magnet. Magnetic. Materials* **428** 368–71
[8] Masrour R, Hlil E K, Hamedoun M, Benyoussef A, Mounkachi O and El Moussaoui H 2015 *J. Magnetism. Magnetic Materials* **378** 37–40
[9] Flemban T H, Singaravelu V, Devi A A S and Roqan I S 2017 *RSC Adv.* **5** 94670–8
[10] Roqan I S, O'Donnell K P, Martin R W, Edwards P R, Song S F, Vantomme A, Lorenz K, Alves E and Boćkowski M 2010 *Phys. Rev.* B **81** 085209
[11] Reehuis M, Krimmel A, Büttgen N, Loidl A and Prokofiev A 2003 *Eur. Phys. J. B-Cond. Matt. Comp. Sys.* **35** 311–16
[12] Jain A *et al* 2013 *APL Mater.* **1** 011002
[13] Alaal N and Roqan I S 2018 *ACS Appl. Nano Mater.* **2** 202–13
[14] Flemban T H, Sequeira M C, Zhang Z, Venkatesh S, Alves E and Lorenz K 2016 *J. Appl. Phys.* **119** 065301
[15] Zhang Z, Schwingenschlögl U and Roqan I S 2014 *J. Appl. Phys.* **116** 183905
[16] Lehmann H W and Harbeke G 1967 *J. App. Phys.* **38** 946
[17] Matsumoto G, Ohbayashi K, Kohn K and Iida S 1966 *J. Phys. Soc. Jpn.* **21** 2429–2429
[18] Thompson S M 2008 The discovery, development and future of GMR: the Nobel Prize 2007 *J. Phys. D: Appl. Phys.* **41** 093001
[19] Hossain A, Seki M, Kawai T and Tabata H 2004 *J. Appl. Phys.* **96** 1273–5
[20] Okamoto S, Ichitsubo T, Kawaguchi T, Kumagai Y, Oba F, Yagi S, Shimokawa K, Goto N, Doi T and Matsubara E 2015 *Adv. Sci.* **2** 1500072
[21] Helmolt V, Wecker R J, Holzapfel B, Schultz L and Samwer K 1993 *Phys. Rev. Lett.* **71** 2331
[22] Mahmood Q, Hassan M, Murtaza G, Sajjad M, Laref A and Haq B 2019 *J. Superconductivity and Novel Magnetism* **32** 1231
[23] Sun X, Bonnick P, Duffort V, Liu M, Rong Z, Persson K A, Ceder G and Nazar L F A 2016 *Energy Environ. Sci.* **9** 2273–7
[24] Allison W, Key B, Phillips P J, Sa N, Lipton A S, Klie R F, Vaughey J T and Poeppelmeier K R 2018 *Inorg. Chem.* **57** 8634–8
[25] Mahmood A, Rashid M, Safder K, Waqas I M, Noor N A, Ramay S M, Masry W A and Al-Garadi N Y A 2021 *Results in Physics* **20** 103709
[26] Blaha P, Schwarz K, Madsen G K H, Kvasnicka D and Luitz J 2001 *WIEN2K, An Augmented Plane Wave + local Orbitals Program for Calculating Crystal Properties, Karlheinz Schwarz* (Austria: Techn. Universiťat Wien)
[27] Koller D, Tran F and Blaha P 2011 Merits and limits of the modified Becke-Johnson exchange potential *Phys. Rev.* B **83** 195134
[28] Madsen G K and Singh D J 2006 BoltzTraP. A code for calculating band-structure dependent quantities *Comput. Phys. Commun.* **175** 67–71
[29] Murnaghan F D 1944 *Proc. Natl. Acad. Sci. U. S. A.* **30** 244–7
[30] Canepa P, Bo S-H, Gautam G S, Key B, Richards W D, Shi T, Tian Y, Wang Y, Li J and Ceder G 2017 *Nat. Commun.* **8** 1759
[31] Noor N A, Hassan M, Rashid M, Alay-e-Abbas S M and Laref A 2017 *Mater. Res. Bull.* **97** 436–43
[32] Tran F and Blaha P 2009 *Phys. Rev. Lett.* **102** 226401
[33] Mustafa G M, Noor N A, Iqbal M W, Sajjad M, Naeem M A, Mahmood Q, Shaikh H M, Mahmood A and Al-Masry W 2020 *Mat. Sci. Sem. Process.* **121** 105452
[34] Wang X, Cheng Z, Wang J and Liu G 2016 *J. Mater. Chem.* C **4** 8535–44
[35] Walsh A, Wai S H, Yan Y, Al-Jassim M M and Turner J A 2007 *Phys. Rev.* B **76** 165119
[36] Yousaf M, Dalhatu S A, Murtaza G, Khenata R, Sajjad M, Musa A, Aliabad H A R and Saeed M A 2015 *J. Alloys and Comp.* **625** 182–7
[37] Mahmood Q, Rashid M, Amin B, Noor N A and Laref A 2019 *Chem. Phys. Lett.* **728** 87–93
[38] Cichy B, Wawrzynczyk D, Samoc M and Stręk W 2017 *J. Mater. Chem.* C **5** 149–58
[39] Yahi H and Meddour A 2017 *J. Magn. Mater.* **432** 591–6
[40] Mahmood Q, Haq B U, Rashid M, Noor N A, AlFaify S and Laref A 2020 *J. Solid State Chem.* **286** 121279
[41] Mahmood Q, Rouf S A, Rashid M, Jamil M, Sajjad M and Laref A 2019 *Z. Naturforsch.* A **74** 1131–8
[42] Khenata R, Rashid M, Noor N A, Sabir B, Ali S, Sajjad M, Hussain F, Khae N U and Amin B 2014 *Comput. Mater. Sci.* **91** 285
[43] Noor N A, Ali S, Murtaza G, Sajjad M, Alay-e-Abbas S M, Shaukat A, Alahmed Z A and Reshak A H 2014 *Comput. Mater. Sci.* **93** 151–9
[44] Tsurkana V, von Nidda H K, Deisenhofer J, Lunkenheimer P and Loidl A 2021 *Phys. Rep.* **926** 1–86
[45] Hassan M, Mahmood Q and Ramay S M 2020 *Mater. Res. Bull.* **123** 110706
[46] Sajjad M, Manzoor S, Zhang H X, Noor N A, Alay-e-Abbas S M, Shaukat A and Khenata R 2014 *J. Supercond. Nov. Magn.* **27** 2327
[47] Sajjad M, Alay-e-Abbas S M, Zhang H X, Noor N A, Saeed Y, Shakir I and Shaukat A 2015 *J. Mag. Mag. Mater.* **390** 78

[48] Sajjad M, Singh N and Larsson J A 2020 *AIP Adv.* **10** 075309
[49] Singh D, Sajjad M, Larsson J A and Ahuja R 2020 *Results in Physics* **19** 103584
[50] Abbas S A, Mahmood I, Sajjad M, Noor N A, Mahmood Q, Naeem M A, Mahmood A and Ramay S M 2020 *Chem. Phys.* **538** 1109022
[51] Aslam M, Khan A, Hashmi M A, Sajjad M, Algrafy E, Mustafa G M, Mahmood A and Ramay S M 2020 *J Mater. Res. Technol.* **9** 9965
[52] Nazir S, Mahmood I, Noor N A, Laref A and Sajjad M 2019 *High Energy Density Phys.* **33** 100715